Zoledronic Acid-Adsorbed Hydroxyapatite and β-Tricalcium Phosphate: Adsorption Efficacy and Cytoprotection In Vitro

Natthawut Laohakulvivat[1], Piyarat Sungkhaphan[2], Boonlom Thavornyutikarn[2], Setthawut Kitpakornsanti[1], Wanida Janvikul[*, 2] and Weerachai Singhatanadgit[*, 1]

[1]Department of Oral and Maxillofacial Surgery, Faculty of Dentistry, Thammasat University, Pathum Thani, Thailand
[2]Biofunctional Materials and Devices Research Group, National Metal and Materials Technology Center, Pathum Thani, Thailand
[*]Corresponding author, E-mail: weerachai.singhatanadgit@gmail.com, wanidaj@mtec.or.th

Abstract

Nowadays, dentists are facing many bisphosphonate-related osteonecrosis of the jaw (BRONJ) patients as the number of patients receiving nitrogen-containing bisphosphonates (N-BPs) is dramatically increasing around the world. One possible cause of BRONJ may involve an increased accumulation of N-BPs to cytotoxic levels in the jawbone. Thus, to reduce the risk of BRONJ, adsorption of unbound N-BP molecules by calcium phosphate adsorbents may help decrease N-BP uptake into the target cells, thus preventing the cytotoxicity of N-BP. The present study aimed to compare the zoledronic acid (ZA) adsorption efficacies of hydroxyapatite (HA) and β-tricalcium phosphate (β-TCP) and to determine the factors influencing their adsorption abilities. Two calcium phosphate adsorbents, i.e., HA and β-TCP, were characterized by scanning electron microscopy (SEM), attenuated total reflection-Fourier transform infrared (ATR-FTIR) and laser light scattering particle size analysis. HA and β-TCP adsorbents, used in various quantities, were individually immersed in the ZA solution as a function of incubation time, to study the ZA adsorption efficacy. The remaining ZA concentration after a given adsorption time was determined using high-performance liquid chromatography (HPLC). The cytoprotection was assessed using an in vitro periodontal ligament (PDL) cells cytotoxicity test. The chemical interaction between each adsorbent and ZA was examined by scanning electron microscopy/energy-dispersive X-ray spectroscopy (SEM/EDX) and ATR-FTIR. The results showed that the particle size distributions of HA and β-TCP were not remarkably different. In terms of ZA adsorption efficacy, 0.02 g of HA possessed the highest adsorption efficiency, approximately 96%, regardless of the adsorption time, whereas 0.005 g of β-TCP showed the lowest efficacy, in the range of approximately 31-41% after 1 h and 24 h of adsorption. The amount of each adsorbent used, but not the adsorption time, seemed to significantly affect the adsorption efficacy. Moreover, a chemical interaction between ZA and HA, but not β-TCP, was likely to occur. It was also found that HA, but not β-TCP, appeared to rescue the number of viable PDL cells, with the 0.02 g HA groups showing the most cytoprotective effects, against ZA regardless of the incubation time. In conclusion, despite the similar shape and size of the particles of the calcium phosphates used, HA provided a much higher ZA adsorption efficiency than β-TCP did, possibly through a higher chemical bonding to ZA. Besides, HA also markedly rescued the cytotoxicity of ZA to PDL cells. It is suggested that HA is a promising bone substitute material candidate for patients with a high risk to develop BRONJ.

Keywords**:** *Cytoprotection, Hydroxyapatite, β-tricalcium phosphate, Zoledronic acid, Adsorption, Periodontal ligament cells*

1. Introduction

Nitrogen-containing bisphosphonates (N-BPs) are antiresorptive drugs used to reduce the risk of skeletal complications in patients suffering from osteoporosis, hypercalcemia, Paget's disease, multiple myeloma, and bone metastasis of cancer (Nicolatou-Galitis et al., 2019; Qayoom et al., 2018; Rasmusson & Abtahi, 2014). N-BPs (both oral and intravenous (IV) forms) are the first-line drugs to treat patients with either osteoporosis or osteopenia as they prevent pathologic fracture of bone (Byun et al., 2017). Nowadays, the number of patients receiving N-BPs has increased, reaching approximately 200 million osteoporosis patients worldwide (Miksad et al., 2011). Therefore, dentists are now facing a challenge in the dental management of patients receiving N-BPs (Nicolatou-Galitis et al., 2019), which may encounter a serious

complication called medication-related osteonecrosis of the jaw (MRONJ or specifically bisphosphonate-related osteonecrosis of the jaw; BRONJ) following routine dental practice involving tooth removal or periodontal surgery. BRONJ is a condition of jawbone necrosis found in patients using N-BPs either oral or IV forms (Salvatore L. Ruggiero et al., 2022). In osteoporosis patients, the risk of developing spontaneous BRONJ is very low but will increase when patients are undergoing osseous surgery or receiving a long course of oral N-BPs for more than 4 years (Salvatore L Ruggiero et al., 2014). In cancer patients receiving N-BP, the incidence of BRONJ is 100 times greater than that in osteoporosis patients due to the higher dose and frequency of IV N-BPs administration (Coleman et al., 2011; Mauri et al., 2009).

The pathogenesis of BRONJ remains unclear. It is widely accepted that this involves the drug cytotoxicity on osteoclast viability and function from high dose N-BPs, thus leading to impairment of bone remodeling and bone healing (Russell, Watts, Ebetino, & Rogers, 2008). To treat BRONJ, supportive treatment is the first choice of treatment with debridement of necrotic bone and antibiotic prescription to prevent further infection. Currently, there are no consensus clinical guidelines or protocols for the management and treatment of BRONJ. The estimated cost for treating BRONJ is about $1,667 per person, and, in the case of surgical intervention, the estimated cost increases to $20,000 per person with a total follow up time of approximately 12 months, and a quarter of BRONJ patients do not improve after receiving the treatment (Najm, Solomon, Woo, & Treister, 2014). It is suggested that a successful preventive measure is necessary.

Several attempts have been made to reduce the risk of BRONJ. Prevention of N-BPs uptake into the target cells could be a promising approach that may reduce the development of BRONJ. It is known that N-BPs bind strongly to hydroxyapatite (HA) in bone and can be released from HA molecules in response to the acidic microenvironment by fully functional osteoclasts during bone repair. The presence of biocompatible adsorbents that have a high affinity to these free (unbound) N-BPs, such as calcium phosphates, is likely to reduce or inactivate free N-BPs up taken by bone cells and soft tissue cells. Previous studies reported the beneficial use of local implantation of synthetic and commercial calcium phosphates such as HA, β-tricalcium phosphate (β-TCP), and biphasic calcium phosphate, to reduce BRONJ in animal models (de Almeida et al., 2018; Paulo et al., 2019; Paulo et al., 2020). As a range of HA to β-TCP ratios in commercial calcium phosphate grafting materials are now available in the market, different forms of calcium phosphates may possess different capacities to adsorb and thus prevent cytotoxicity of zoledronic acid (ZA), the most potent N-BPs widely used in patients. Strong evidence about the efficacies of HA and β-TCP in adsorbing ZA and the regulation of their adsorption is, however, very limited.

2. Objectives

The present study, therefore, aimed to compare the ZA adsorption and cytoprotection efficacies between HA and β-TCP. Factors influencing their adsorption abilities, *i.e.*, amount of adsorbent and incubation time, were also determined.

3. Materials and Methods

Two different calcium phosphate (CaP) adsorbents, i.e., hydroxyapatite (HA) and β-tricalcium phosphate (β-TCP), were used in the present study. HA was purchased from Taihei Chemical Industrial Co., Ltd., (CAS.No. 1306-06-5), and β-TCP was obtained from Merck German (CAS. No. 7758-87-4). Characterization of adsorbents, determination of ZA adsorption efficiency, analysis of ZA-adsorbent interaction, and cytotoxicity testing are described below.

3.1 Scanning electron microscopy (SEM)

SEM was used to examine the morphological features of HA and β-TCP particles. The samples were prepared by dispersing each sample powder in 100% ethanol, after which aliquots of 5 µL of each slurry were dropped on coverslips. The samples were dried at room temperature for 30 min. The conductive coating was done by gold coating, and SEM was carried out using a scanning electron microscope (JCM-6000, JEOL Ltd., Tokyo, Japan). The accelerating voltage was set at 15 kV. The contrast and brightness of

the images were adjusted to optimal values so that the particles could be easily distinguished from the background. Images (a magnification at 2000X) were used for image acquisition and analysis.

3.2 Analysis of particle size distribution

The particle size distributions and the mean particle sizes of HA and β-TCP powders were measured by using a laser light scattering particle size analyzer (Mastersizer-2000, Malvern Instruments, Great Malvern, UK). Briefly, 0.5 mg of each of the dried samples was suspended in 20 mL of deionized (DI) water and then stirred for 4 min with high-speed spinning. The mean diameters of the individual analyzed adsorbents were reported along with the corresponding percentile values, i.e., D10, D50, and D90, read from the corresponding cumulative particle size distributions.

3.3 ZA adsorption assay

Zoledronic acid monohydrate powder (Tokyo Chemical Industry Co., Ltd., CAS.No. 165800-06-6) was reconstituted in deionized (DI) water to obtain a 100 µM ZA solution. The solution was filtered through a 0.22 µm nylon filter. 0.005 g and 0.02 g of both HA and β-TCP powders were sterilized with 70% ethanol and then extensively washed in DI water 3 times. The powders were separately incubated in 1 mL of 100 µM ZA at 37°C to allow the adsorption for 1 h and 24 h under an orbital rotator at a constant speed of 5 rpm. 0.02 g of HA and β-TCP individually incubated in DI water for 24 h were also used as controls. After each time point, the samples were centrifuged (Eppendorf® Centrifuge 5415R, Eppendorf AG, Hamburg, Germany) at 10000 rpm for 10 min, and the supernatant in each sample was collected for cytotoxicity testing. The pelleted powder samples were dried at 60°C for 24 h, and half of each sample was further washed extensively in DI water 3 times to eliminate any ZA physically adsorbed on the sample before drying at 60°C for 24 h. All powder samples collected both before and after extensive washing were stored in a desiccator before being analyzed.

3.4 High-performance liquid chromatography (HPLC)

HPLC was used to examine the amount of ZA remaining in each supernatant after each adsorption was performed. The collected supernatants were individually filtered through 0.22 µm nylon filters, and the amounts of ZA were subsequently measured using HPLC (WATERS HPLC 2965 SYSTEM) with FRC-10A Fraction Collector (Shimadzu) under the following conditions; Column 250 x 3.0 mm^2, Temperature 30°C, Time 10 min, Flow rate: 1.0 $mL \cdot min^{-1}$, Detection: 210 nm using a UV detector, Injection volume 50 µL, Diluent: mobile phase (phosphate buffer: methanol 90:10 v/v). The amount of ZA found in each sample was calculated based on a standard calibration curve constructed using six known ZA concentrations (10, 20, 40, 60, 80, and 100 µM). The initial amount of ZA used and the remaining amount of ZA determined was promptly employed for the assessment of the adsorption efficiency of the tested adsorbent under a given adsorption condition studied.

3.5 Scanning electron microscopy/energy-dispersive X-ray spectroscopy (SEM/EDX)

The mass level of nitrogen, indicative of the presence of adsorbed N-BPs, found on the adsorbent surface directly corresponds to the amount of ZA adsorbed. HA and β-TCP that showed the highest adsorption efficacy were used as candidate representatives for SEM/EDX analysis, which was investigated using SEM (HITACHI S3400N, Hitachi, Ltd., Chiyoda, Japan) equipped with an EDX attachment operating at 20 kV, a working distance of 10 mm, and an image magnification of 2000X. The elemental analysis using TEAM™ Analysis System (EDEN Instruments SAS, Valence, France) was performed on 5-7 sample spots per field in each sample, and the average weight percent of nitrogen was later calculated.

3.6 Attenuated total reflection - Fourier transform infrared (ATR-FTIR)

ATR-FTIR was used to observe any newly formed chemical bonds between the molecules of ZA and each adsorbent as well as any changes in the chemical bonds of the adsorbent molecules after the adsorption process. Briefly, 5 mg of HA and β-TCP powders were individually incubated with 100 µL of 1 mM ZA at room temperature for 1 h (the relatively high concentration of ZA was used to obtain sufficiently

high IR signals for detection). Subsequently, the samples were dried at 60°C overnight and then subjected to ATR-FTIR measurement. FTIR spectra were recorded over a 400-4000 cm^{-1} range using a Nicolet™ iS™ 5 FTIR Spectrometer (Thermo Fisher Scientific, Massachusetts, USA). The spectral resolution was 4 cm^{-1} and 32 scans per spectrum. The data was analyzed using OriginPro 8.5.0 software (Originlab corporation, Massachusetts, USA). Pure ZA, HA, and β-TCP powders and combinations of dried powders between each adsorbent and ZA were also analyzed as references.

3.7 In vitro cytotoxicity test

To investigate the cytoprotective effects of HA and β-TCP against the cytotoxicity of ZA, the effect of remaining ZA in each solution after adsorption by HA or β-TCP on the number of viable human periodontal ligament (PDL) cells was determined. The use of PDL cells was approved by the Human Research Ethics Committee of Thammasat University (Science) (COA NO. 068/2564) and the Thammasat University Biosafety Committee (NO. 057/2564). Briefly, 200 µL of each of the supernatants obtained in section 3.4 was mixed (1:1) with 2X Dulbecco's Modified Eagle Medium (DMEM) containing 20% fetal bovine serum (FBS), penicillin-streptomycin (10,000 U/mL) (all from Gibco Life Technologies Ltd, Paisley, UK). Each diluted ZA supernatant was used to treat PDL cells (which were previously seeded at a density of $5x10^4$ cell/well in a 96-well plate at 37°C) for 96 h at 100% relative humidity and 5% CO_2. After 96 h, all samples were fixed with 4% paraformaldehyde (PFA), and 4',6-diamidino-2-phenylindole (DAPI) staining was carried out to measure the number of viable adherent PDL cells using ImageJ software (NIH, USA).

3.8 Statistical analysis

Adsorption efficacy, percent weight of nitrogen component, and viable cells in DAPI staining of each sample were presented as the mean ± S.D. obtained from at least 5 replicates. The distribution of data was evaluated by the Kolmogorov-Smirnov test. Levene's test for equality of variances was shown non-homogeneity of variance. Welch's ANOVA and Games-Howell post-hoc analysis were used to analyze the data. Pearson correlation was used to study the correlation between the adsorbent amount and adsorption time on the number of viable cells. Statistical analysis was performed using IBM SPSS Software Version 22 (International Business Machines Corporation, New York, USA), with $p < 0.05$ considered statistically significant.

4. Results and Discussion

4.1 Results

4.1.1 Characterization of HA and β-TCP adsorbents

SEM images in Figures 1a and 1b reveal the particle agglomeration of HA and β-TCP, respectively. Both HA and β-TCP particles apparently possessed irregular shapes and various sizes. The ATR-FTIR spectra of HA and β-TCP adsorbents are shown in Figure 1c. The characteristic absorption peaks of HA were found at the following wavenumbers: 472, 560, 600, 632, 874, 960,1015, 1085, 1415, 1453, 2338, and 2360 cm^{-1} (Ozhukil Kollath et al., 2015). The peaks at 874 and around 1415 to 1453 cm^{-1} represent υ2 and υ3 bands of carbonate ions, respectively, due to the carbonate substitution for hydroxyl and phosphate groups in HA that may occur during the manufacturing process (LeGeros, Trautz, Klein, & LeGeros, 1969). The phosphate groups were detected at the ranges of 472-632 cm^{-1}, representing a υ4 vibration mode of PO_4^{3-}, and 960-1085 cm^{-1}, representing υ1 and υ3 vibration modes of PO_4^{3-}. On the other hand, the characteristic absorption peaks of β-TCP were found at the following wavenumbers: 495, 540, 588, 602, 668, 725, 942, 968, 1001, 1100, 1115, 1187, 1121 cm^{-1} (Tavares Ddos, Castro Lde, Soares, Alves, & Granjeiro, 2013). The peaks around 495-725 cm^{-1} represent a υ4 vibration mode of PO_4^{3-}, whereas those around 942-1121 cm^{-1} represent a υ3 vibration mode of PO_4^{3}.

From the particle size analysis results shown in Table 1, the sizes below 10%, 50%, and 90% of all HA particles found were 2.36, 6.81, and 14.98 µm, respectively, while those of β-TCP particles were 1.15,

4.34, and 14.20 µm, respectively. The particle size distributions of these two adsorbents were not remarkably different.

4.1.2 Adsorption efficacies of HA and β-TCP adsorbents

The amount of ZA remaining in each supernatant after certain adsorption was analyzed using HPLC in order to determine the adsorption efficacy of a given adsorbent (Table 2). When HA was used at 0.005 g and 0.02 g HA to adsorb 100 µM ZA for 1 and 24 h, the adsorption efficacy of HA was slightly raised with an increase in the quantity of the adsorbent used. Moreover, it could instantly absorb ZA; a prolonged adsorption time barely increased the amount of ZA adsorbed. Overall, HA could adsorb ZA quite efficiently; its adsorption efficacy was in the range of 80-96%. In contrast, β-TCP demonstrated a considerably lower adsorption efficacy, especially when a small quantity of the adsorbent was in use. When a higher amount, i.e., 0.02 g of β-TCP was employed, its adsorption efficacy was raised approximately two folds, with respect to that of β-TCP used at 0.005 g. Although the adsorption rate seemed to escalate slightly as a function of adsorption time, the adsorption efficacy of β-TCP was, overall, only in the range of 31-85%.

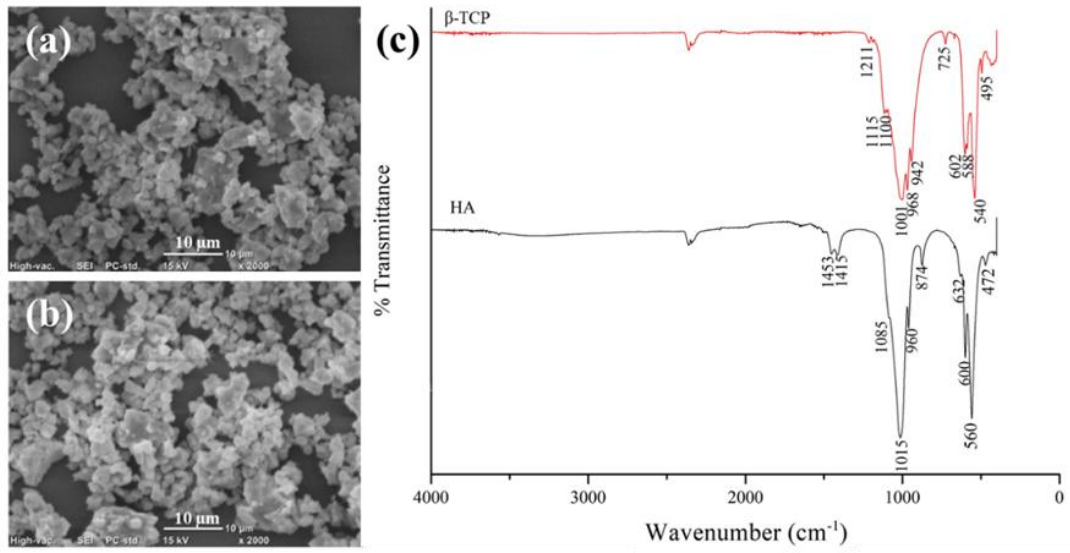

Figure 1 The characterization results of HA and β-TCP adsorbents.
SEM images of (a) HA and (b) β-TCP. (c) FTIR spectra of HA and β-TCP.

Table 1 The particle size distributions of HA and β-TCP powders analyzed by a laser light scattering technique

Percentile value	Particle size (µm)	
	HA	β-TCP
D10	2.36	1.15
D50	6.81	4.34
D90	14.98	14.20

4.1.3 Binding of ZA to HA or β-TCP adsorbents

ATR-FTIR was used to investigate the chemical binding of ZA to each of the adsorbents exploited. In Figures 2a and 2b, the spectrum of ZA-adsorbed HA (denoted as HA + ZA solution (HA bonded) in Figures 2a and 2b) clearly demonstrates the shifted wavenumbers of the absorption bands from 560 to 565 cm^{-1} (υ4 vibration mode of PO_4^{3-} in HA molecule), 1024 to 1021 cm^{-1} (υ3 vibration mode of PO_4^{3-} in HA molecule), 624 to 629 cm^{-1} (υ4 vibration mode of PO_4^{3-} in ZA) and 1091 to 1086 cm^{-1} (C-O stretching in

ZA), with respect to the wavenumbers of those absorption bands of a mixture of HA and ZA powders (denoted as HA + ZA powder (HA unbonded) in Figures 2a and 2b), suggesting a possible chemical interaction between ZA and HA upon adsorption. In contrast, no spectral shifts were observed in the ZA-adsorbed β-TCP (Figure 2c and 2d); the absorption bands of both β-TCP + ZA solution (β-TCP bonded) and β-TCP + ZA powder (β-TCP unbounded) were observed at similar wavenumbers.

Table 2 The adsorption efficacies of HA and β-TCP adsorbents incubated with 100 µM ZA at varied amounts of adsorbents and incubation times used

Adsorbent	Amount (g)	Time (h)	Remaining ZA concentration (mean ± S.D.; µM)	Adsorption efficacy (% mean ± S.D.)
HA	0.005 g	1 h	17.69 ± 3.35	82.33 ± 2.31
		24 h	19.71 ± 4.16	80.74 ± 2.46
	0.02 g	1 h	3.20 ± 0.06	96.78 ± 0.17
		24 h	3.11 ± 0.02	96.87 ± 0.23
β-TCP	0.005 g	1 h	68.25 ± 0.58	31.26 ± 5.18
		24 h	58.34 ± 2.00	41.35 ± 2.24
	0.02 g	1 h	25.77 ± 6.55	74.83 ± 4.27
		24 h	14.63 ± 3.71	85.43 ± 2.83

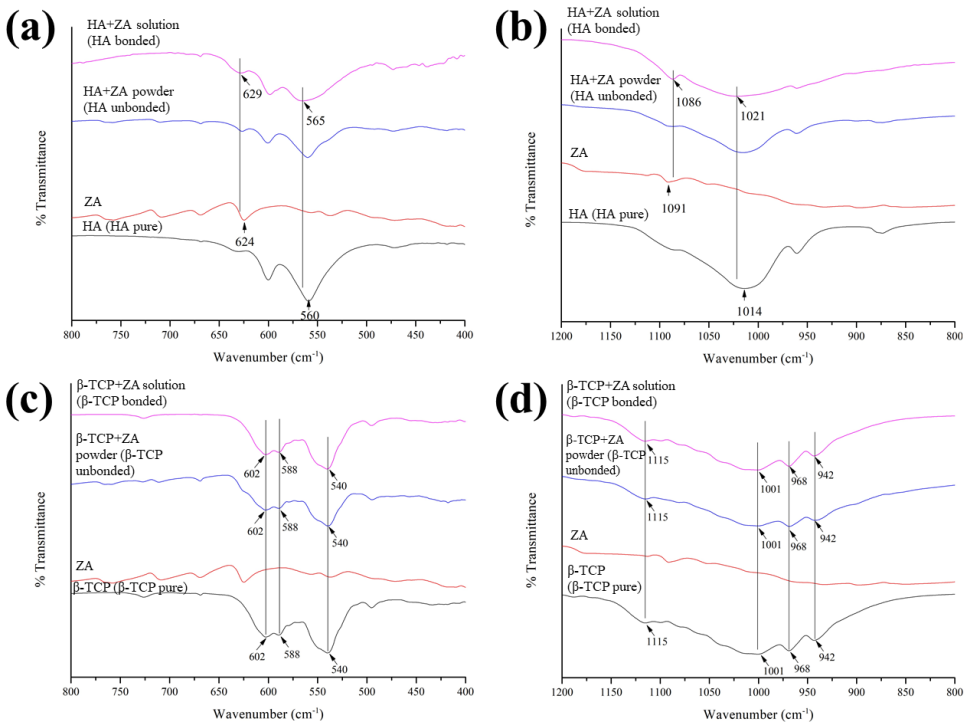

Figure 2 The overlaid ATR-FTIR spectra of HA incubated with a ZA solution, HA mixed with a ZA powder, pure ZA, and pure HA at the different wavenumber ranges: (a) 400-800 cm^{-1} and (b) 800-1200 cm^{-1}. The overlaid spectra of β-TCP incubated with a ZA solution, β-TCP mixed with a ZA powder, pure ZA, and pure β-TCP at the wavenumber ranges: (c) 400-800 cm^{-1} and (d) 800-1200 cm^{-1}.

In Figure 3, the SEM-EDX elemental analysis results from the HA and β-TCP groups that showed the highest adsorption efficacy from data shown in Table 2 (0.02 g HA 24 hours and 0.02 g β-TCP 24 hours) vividly confirmed the chemical adsorption of ZA onto the HA particles; after extensive rinsing with DI water, the presence of ZA, identified by the detection of nitrogen element by EDX, in the ZA-adsorbed HA particles was positively verified. The mean weight percentages of nitrogen found in the ZA-adsorbed HA samples before and after purification were 0.23 ± 0.19 and 0.18 ± 0.15, respectively (Figures 3a and 3b). The results acquired from EDX analysis also indicated no chemical interaction between β-TCP and ZA dissolved in the solution; a trace of nitrogen detected in the ZA-adsorbed β-TCP sample prior to successive washing with DI water entirely disappeared after washing (Figures 3c and 3d).

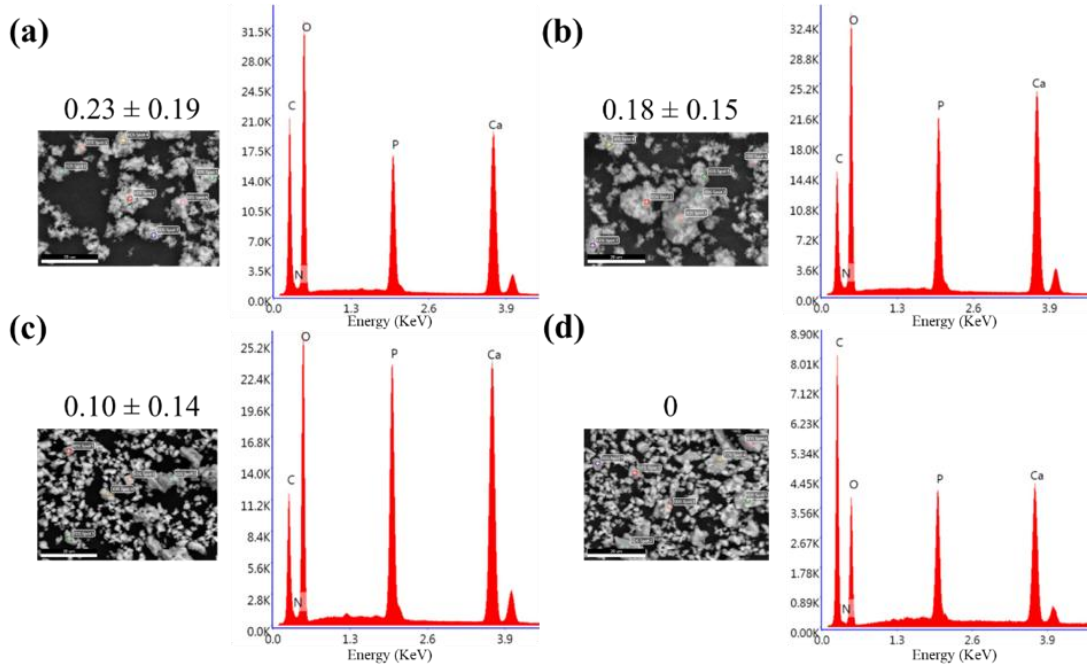

Figure 3 The EDX spectra of ZA-adsorbed HA (0.02 g HA, 24 h group) (a and b) and ZA-adsorbed β-TCP (0.02 g β-TCP, 24 h group) (c and d) before and after extensive washing with DI water, respectively. The mean nitrogen content (% weight) ± S.D. determined from each sample is reported on the top of the corresponding SEM image.

4.1.4 Cell viability

The results in Figure 4a reveal that the supernatants from HA and β-TCP slurries had no cytotoxicity, whereas pure ZA solution, without any adsorbents, was highly cytotoxic. Apparently, HA, but not β-TCP, particularly when used at 0.02 g, was able to significantly rescue the number of viable cells. Interestingly, the cytoprotective effect of HA against ZA was explicitly noticed, regardless of the ZA/HA adsorption time. Besides, HA prevented ZA-induced apoptosis of PDL cells, whereas a number of apoptotic DNA fragmentation (white arrows) were observed in the β-TCP group (Figure 4b). A summary of the cytotoxicity results is shown in Figure 4c. Pearson correlation analysis showed no relation between the number of viable cells count and adsorption time (p = 0.307). In contrast, the amount of HA adsorbent demonstrated a positive strong correlation with the number of viable cells (p = 0.000, r = 0.882).

4.2 Discussion

Effective prevention of BRONJ is currently required. Calcium phosphate bone substitutes have been suggested to adsorb N-BPs and reduce the risk to develop BRONJ (de Almeida et al., 2018; Paulo et al., 2019; Paulo et al., 2020). The present study compared the ZA adsorption abilities of HA and β-TCP, the

two most commonly used synthetic bone substitutes, and, thus, their cytoprotection against ZA. The results showed that although both HA and β-TCP could adsorb ZA, HA possessed a higher ZA adsorption ability and, thus, greater cytoprotection.

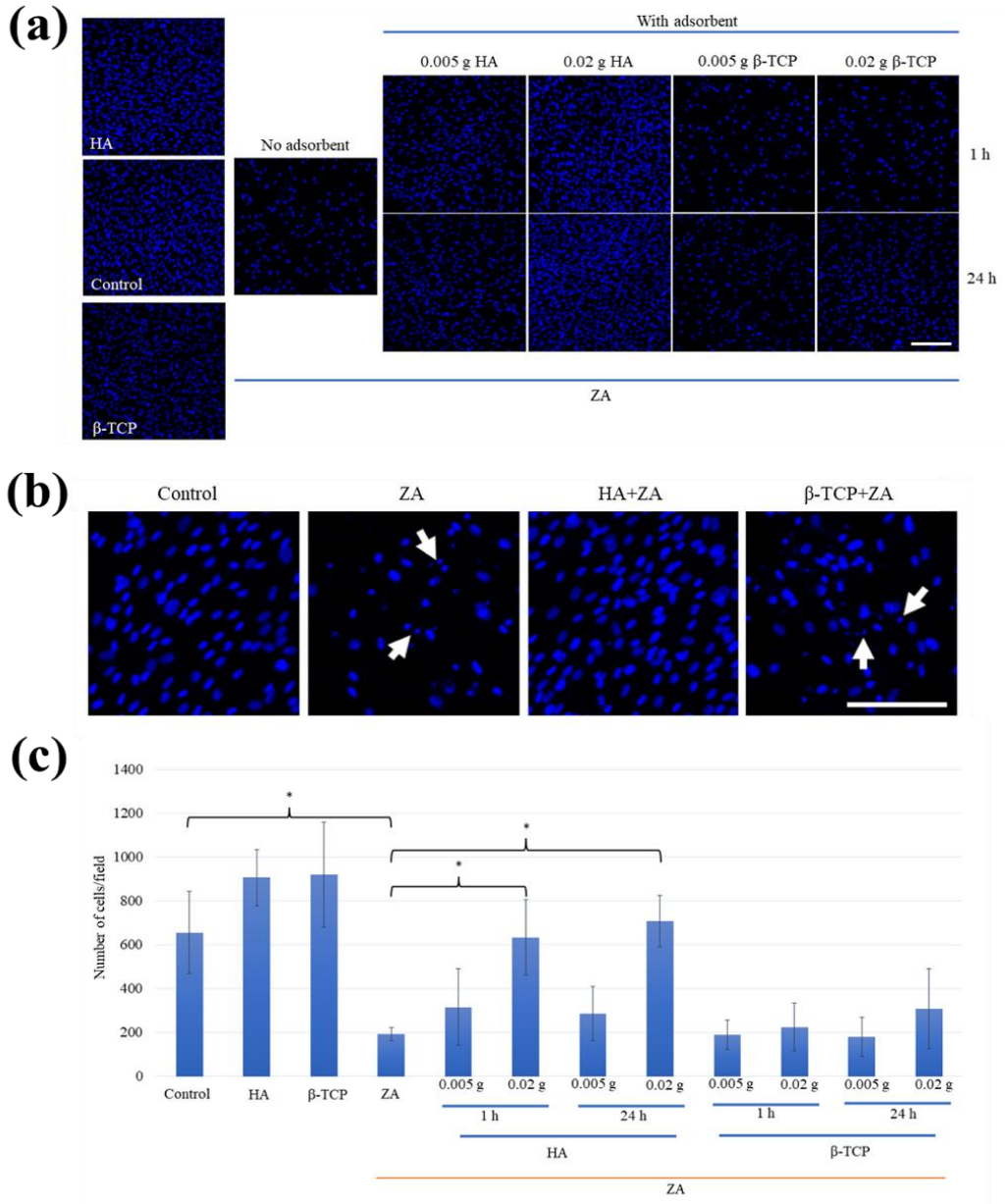

Figure 4 DAPI staining of viable PDL cells treated with various ZA solutions previously incubated with different amounts of HA or β-TCP adsorbents for 1 h and 24 h. (a) Untreated cells and cells treated with ZA-free solutions previously incubated with HA or β-TCP were used as controls. (b) The apoptotic cells are indicated by the white arrows in each condition. Scale bar = 100 µm. (c) The number of viable PDL cells treated with various ZA solutions previously incubated with different amounts of HA or β-TCP adsorbents for 1 h and 24 h. The results show the mean cells number/field (± S.D.) from 9 fields. *$p < 0.05$.

Previous studies on the chemical bonding of ZA to HA have established that the P-C-P structure of N-BPs plays an important role in the chemical bonding (Boanini, Gazzano, & Bigi, 2012; Lawson et al., 2010; Nancollas et al., 2006; Qiu et al., 2013). Calcium is a bone mineral that interacts with the phosphate groups of N-BPs. Both HA and β-TCP have calcium in their molecules. However, the chemical bonding between ZA and each of the calcium phosphate adsorbents used in the present study was only observed in HA, but not in β-TCP. Some FTIR absorption peaks of the ZA-adsorbed HA specimen shifted, with respect to those of the mixture of HA and ZA powders as evidently seen in Figure 2. These shifts were likely attributed to the chemical interaction between HA and ZA via ionic bond forming between calcium ions in HA molecule (blue boxes in Figure 5) and hydroxyl (-OH) groups, i.e., both in phosphate groups (red box) and a free -OH group (green box) adjacent to the P-C-P ligand, in ZA, as reported previously (Li et al., 2017). Although calcium is also presented in β-TCP, the present study could not observe any chemical interaction between β-TCP and ZA since there were no spectral shifts in the FTIR spectrum of the ZA-adsorbed β-TCP specimen. Moreover, the EDX result indicated the absence of ZA in the ZA-adsorbed β-TCP specimen after washing with DI water successively. It is possible that under an acidic solution of ZA, β-TCP likely underwent degradation more rapidly than HA did (Kameda, Aizawa, Sato, & Honda, 2021; LeGeros, 2002), and the adsorbed ZA/calcium complex was in turn dissolved back into the solution, resulting in cytotoxicity to PDL cells (Cao, Chen, & Schreyer, 2012; Kameda et al., 2021; Kass & Orrenius, 1999). It is noteworthy that in the control β-TCP incubated with ZA-free solutions, the number of viable cells appeared unaffected, which can be due to a neutral pH of the ZA-free solutions that did not cause rapid degradation of β-TCP as observed in the acidic ZA solution (Kameda et al., 2021). Furthermore, the particle size distributions of HA and β-TCP used in the present study were not much different, as determined by the laser light scattering analysis. A superior ZA adsorption efficacy of HA was, therefore, unlikely due to a difference in the physical adsorption. The explanation why HA was more effective in adsorption of ZA than β-TCP would only be described by the chemical binding between ZA and HA as well as the less susceptibility to degradation of HA in the acidic solution of ZA. Further studies are undoubtedly suggested to thoroughly investigate the actual causes of a lower ZA adsorption efficacy of β-TCP when compared with that of HA.

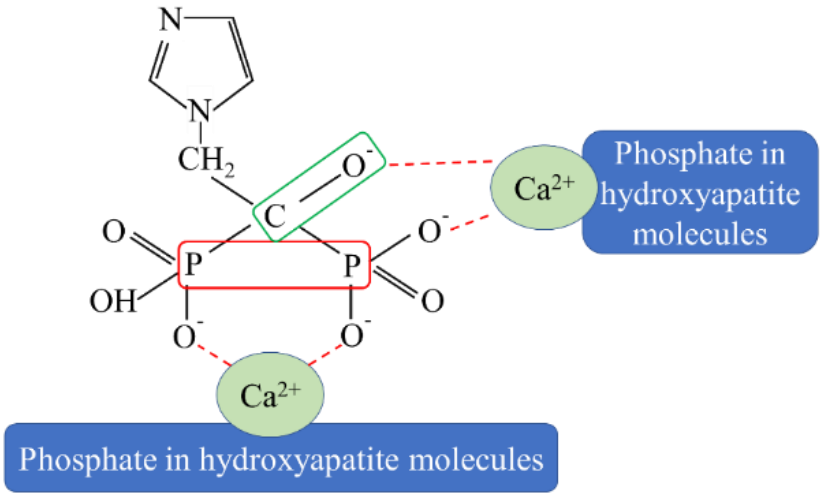

Figure 5 The chemical interaction between ZA and HA via ionic bond forming between calcium ions in HA and hydroxyl groups in ZA

Cytoprotective effects of the tested adsorbents against ZA were determined using an in vitro human PDL cells model. PDL tissue components have been shown to remain in the human extraction socket for 2 weeks post-extraction (Devlin & Sloan, 2002), and PDL cells have also been suggested to play a role in the healing of the extraction socket (Lin, McCulloch, & Cho, 1994; Loo-Kirana, Gilijamse, Hogervorst, Schoenmaker, & de Vries, 2021; Pei et al., 2017). In the present study, complete cytoprotection against ZA was only observed in the 0.02 g HA groups (Table 2). The remaining ZA concentrations in these groups, at 1 and 24 h, were approximately 3 μM, which is lower than the previously reported toxic dose (5 μM) (Patntirapong, Singhatanadgit, Chanruangvanit, Lavanrattanakul, & Satravaha, 2012). Moreover, HA was also able to inhibit cells apoptosis, as indicated by the presence of DNA fragmentation shown in Figure 4b in the present study. Cells apoptosis has been shown to play an important role in ZA cytotoxicity to hMSCs (Singhatanadgit, Hankamolsiri, & Janvikul, 2021), which strongly supports a cytoprotective role of HA adsorbent against ZA.

The concentration of ZA used in this study was based on the physiological range detected in resorption lacunae in vivo (10-100 μM) (Sato et al., 1991; Vaisman, McCarthy, & Cortizo, 2005), and bone from patients with existing osteonecrosis of the jaw (ONJ) showed estimated levels of ZA ranging from 0.4 to 4.6 μM (Scheper et al., 2009). A volume of an extraction socket ranges between 0.5 and 1 mL in a single-root tooth and a multi-root tooth (Thousand, Datar, Font, & Powell, 2017). The amounts of HA and β-TCP in the present study, which are equivalent to 0.5-1 mL are approximately 0.16-0.32 g and 0.33-0.66 g, respectively. Based on the present results, 0.16-0.32 g HA in a single-root tooth and a multi-root tooth can adsorb ZA 1.9 mM, which is much higher than the highest previously reported accumulated ZA concentration in the BRONJ extraction socket (Wen, Qing, Harrison, Golub, & Akintoye, 2011).

The main limitations of the present study are the limited variation of each variable studied. We determined the effect of two quantities of the adsorbents, two adsorption times, and one concentration of ZA on the adsorption efficacies and cytoprotective potentials of the calcium phosphates. The lower ZA adsorption efficacy of β-TCP, when compared with that of HA, could not be unequivocally claimed. The adsorption of ZA to β-TCP has possibly not reached its maximum capacity with the adsorption time used in the study. To better understand the adsorption kinetic, equilibrium information, and maximum adsorption capacity of the adsorbents, more experiments considering a range of variations of each variable are needed. Varying the adsorption times, the amounts of adsorbent, and the initial concentrations of ZA should be considered in future studies, which will also provide detailed information regarding the mechanisms mediating the ZA adsorption roles of the calcium phosphate adsorbents and significant factors controlling this process. Besides, commonly used characterization techniques were applied in the present study. The limited sensitivity of such techniques may not be sufficient to thoroughly characterize subtle changes in the chemical properties of the ZA-adsorbed calcium phosphates. For example, highly sensitive methods or additional techniques, such as CHN elemental analysis, may be used to evaluate the chemical adsorption of the adsorbent to support SEM/EDX results. It is also possible that a small amount of ZA chemically adsorbed on the surface of β-TCP could not be detected by ATR-FTIR in the present study. The proof of β-TCP degradation is not provided in the present study whilst it should be carried out to support possible different ZA adsorption kinetics of HA and β-TCP. Further studies are warranted.

5. Conclusions

In conclusion, despite similar shapes and sizes of the particles of the calcium phosphates studied, HA was proven to provide a quite higher ZA adsorption efficiency than β-TCP did, possibly through a higher (chemical) interaction between ZA and HA. Besides, HA markedly rescued the cytotoxicity of ZA to PDL cells. It is suggested that HA is a promising bone substitute material candidate for patients with a high risk to develop BRONJ.

6. Acknowledgement

This research was supported by the Thailand Graduate Institute of Science and Technology (TGIST), National Science and Technology Development Agency (SCA-CO-2564 14581 TH).

7. References

Boanini, E., Gazzano, M., & Bigi, A. (2012). Time Course of Zoledronate Interaction with Hydroxyapatite Nanocrystals. *The Journal of Physical Chemistry C, 116*(29), 15812-15818. doi:10.1021/jp304472s

Byun, J. H., Jang, S., Lee, S., Park, S., Yoon, H. K., Yoon, B. H., & Ha, Y. C. (2017). The efficacy of bisphosphonates for prevention of osteoporotic fracture: an update meta-analysis. *J Bone Metab, 24*(1), 37-49. doi:10.11005/jbm.2017.24.1.37

Cao, N., Chen, X. B., & Schreyer, D. J. (2012). Influence of Calcium Ions on Cell Survival and Proliferation in the Context of an Alginate Hydrogel. *ISRN Chemical Engineering, 2012*, 516461. doi:10.5402/2012/516461

Coleman, R., Woodward, E., Brown, J., Cameron, D., Bell, R., Dodwell, D., . . . Thorpe, H. (2011). Safety of zoledronic acid and incidence of osteonecrosis of the jaw (ONJ) during adjuvant therapy in a randomised phase III trial (AZURE: BIG 01-04) for women with stage II/III breast cancer. *Breast Cancer Res Treat, 127*(2), 429-438. doi:10.1007/s10549-011-1429-y

de Almeida, A. D., Leite, F. G., Chaud, M. V., Rebelo, M. A., Borges, L., Viroel, F. J. M., . . . Grotto, D. (2018). Safety and efficacy of hydroxyapatite scaffold in the prevention of jaw osteonecrosis in vivo. *J Biomed Mater Res B Appl Biomater, 106*(5), 1799-1808. doi:10.1002/jbm.b.33995

Devlin, H., & Sloan, P. (2002). Early bone healing events in the human extraction socket. *Int J Oral Maxillofac Surg, 31*(6), 641-645. doi:10.1054/ijom.2002.0292

Kameda, Y., Aizawa, M., Sato, T., & Honda, M. (2021). Zoledronic Acid-Loaded beta-TCP Inhibits Tumor Proliferation and Osteoclast Activation: Development of a Functional Bone Substitute for an Efficient Osteosarcoma Treatment. *Int J Mol Sci, 22*(4). doi:10.3390/ijms22041889

Kass, G. E., & Orrenius, S. (1999). Calcium signaling and cytotoxicity. *Environmental health perspectives, 107 Suppl 1*(Suppl 1), 25-35. doi:10.1289/ehp.99107s125

Lawson, M. A., Xia, Z., Barnett, B. L., Triffitt, J. T., Phipps, R. J., Dunford, J. E., . . . Russell, R. G. (2010). Differences between bisphosphonates in binding affinities for hydroxyapatite. *J Biomed Mater Res B Appl Biomater, 92*(1), 149-155. doi:10.1002/jbm.b.31500

LeGeros, R. Z. (2002). Properties of osteoconductive biomaterials: calcium phosphates. *Clin Orthop Relat Res*(395), 81-98. doi:10.1097/00003086-200202000-00009

LeGeros, R. Z., Trautz, O. R., Klein, E., & LeGeros, J. P. (1969). Two types of carbonate substitution in the apatite structure. *Experientia, 25*(1), 5-7. doi:10.1007/bf01903856

Li, W., Xin, X., Jing, S., Zhang, X., Chen, K., Chen, D., & Hu, H. (2017). Organic metal complexes based on zoledronate–calcium: a potential pDNA delivery system. *Journal of Materials Chemistry B, 5*(8), 1601-1610. doi:10.1039/C6TB03041F

Lin, W. L., McCulloch, C. A., & Cho, M. I. (1994). Differentiation of periodontal ligament fibroblasts into osteoblasts during socket healing after tooth extraction in the rat. *Anat Rec, 240*(4), 492-506. doi:10.1002/ar.1092400407

Loo-Kirana, R., Gilijamse, M., Hogervorst, J., Schoenmaker, T., & de Vries, T. J. (2021). Although Anatomically Micrometers Apart: Human Periodontal Ligament Cells Are Slightly More Active in Bone Remodeling Than Alveolar Bone Derived Cells. *Frontiers in Cell and Developmental Biology, 9*. doi:10.3389/fcell.2021.709408

Mauri, D., Valachis, A., Polyzos, I. P., Polyzos, N. P., Kamposioras, K., & Pesce, L. L. (2009). Osteonecrosis of the jaw and use of bisphosphonates in adjuvant breast cancer treatment: a meta-analysis. *Breast Cancer Res Treat, 116*(3), 433-439. doi:10.1007/s10549-009-0432-z

Miksad, R. A., Lai, K.-C., Dodson, T. B., Woo, S.-B., Treister, N. S., Akinyemi, O., . . . Gazelle, G. S. (2011). Quality of life implications of bisphosphonate-associated osteonecrosis of the jaw. *The oncologist, 16*(1), 121.

Najm, M. S., Solomon, D. H., Woo, S. B., & Treister, N. S. (2014). Resource utilization in cancer patients with bisphosphonate- associated osteonecrosis of the jaw. *Oral diseases, 20*(1), 94-99.

Nancollas, G. H., Tang, R., Phipps, R. J., Henneman, Z., Gulde, S., Wu, W., . . . Ebetino, F. H. (2006). Novel insights into actions of bisphosphonates on bone: differences in interactions with hydroxyapatite. *Bone, 38*(5), 617-627. doi:10.1016/j.bone.2005.05.003

Nicolatou-Galitis, O., Schiodt, M., Mendes, R. A., Ripamonti, C., Hope, S., Drudge-Coates, L., . . . Van den Wyngaert, T. (2019). Medication-related osteonecrosis of the jaw: definition and best practice for prevention, diagnosis, and treatment. *Oral Surg Oral Med Oral Pathol Oral Radiol, 127*(2), 117-135. doi:10.1016/j.oooo.2018.09.008

Ozhukil Kollath, V., Van den Broeck, F., Feher, K., Martins, J. C., Luyten, J., Traina, K., . . . Cloots, R. (2015). A Modular Approach To Study Protein Adsorption on Surface Modified Hydroxyapatite. *Chemistry, 21*(29), 10497-10505. doi:10.1002/chem.201500223

Patntirapong, S., Singhatanadgit, W., Chanruangvanit, C., Lavanrattanakul, K., & Satravaha, Y. (2012). Zoledronic acid suppresses mineralization through direct cytotoxicity and osteoblast differentiation inhibition. *Journal of oral pathology & medicine, 41*(9), 713-720. doi:https://doi.org/10.1111/j.1600-0714.2012.01154.x

Paulo, S., Laranjo, M., Abrantes, A. M., Casalta-Lopes, J., Santos, K., Goncalves, A. C., . . . Ferreira, M. M. (2019). Synthetic calcium phosphate ceramics as a potential treatment for bisphosphonate-related osteonecrosis of the jaw. *Materials (Basel), 12*(11). doi:10.3390/ma12111840

Paulo, S., Laranjo, M., Paula, A., Abrantes, A. M., Martins, J., Marto, C. M., . . . Marques Ferreira, M. (2020). Calcium phosphate ceramics can prevent bisphosphonate-related osteonecrosis of the jaw. *Materials (Basel), 13*(8). doi:10.3390/ma13081955

Pei, X., Wang, L., Chen, C., Yuan, X., Wan, Q., & Helms, J. A. (2017). Contribution of the PDL to Osteotomy Repair and Implant Osseointegration. *Journal of dental research, 96*(8), 909-916. doi:10.1177/0022034517707513

Qayoom, I., Raina, D. B., Sirka, A., Tarasevicius, S., Tagil, M., Kumar, A., & Lidgren, L. (2018). Anabolic and antiresorptive actions of locally delivered bisphosphonates for bone repair: A review. *Bone Joint Res, 7*(10), 548-560. doi:10.1302/2046-3758.710.BJR-2018-0015.R2

Qiu, L., Lin, J., Wang, L., Cheng, W., Cao, Y., Liu, X., & Luo, S. (2013). A Series of Imidazolyl-Containing Bisphosphonates with Abundant Hydrogen-Bonding Interactions: Syntheses, Structures, and Bone-Binding Affinity. *Australian Journal of Chemistry, 67*, 192-205.

Rasmusson, L., & Abtahi, J. (2014). Bisphosphonate associated osteonecrosis of the jaw: an update on pathophysiology, risk factors, and treatment. *International Journal of Dentistry, 2014*, 471035. doi:10.1155/2014/471035

Ruggiero, S. L., Dodson, T. B., Aghaloo, T., Carlson, E. R., Ward, B. B., & Kademani, D. (2022). American Association of Oral and Maxillofacial Surgeons' Position Paper on Medication-Related Osteonecrosis of the Jaw – 2022 Update. *Journal of oral and maxillofacial surgery*. doi:https://doi.org/10.1016/j.joms.2022.02.008

Ruggiero, S. L., Dodson, T. B., Fantasia, J., Goodday, R., Aghaloo, T., Mehrotra, B., & O'Ryan, F. (2014). American Association of Oral and Maxillofacial Surgeons position paper on medication-related osteonecrosis of the jaw—2014 update. *Journal of oral and maxillofacial surgery, 72*(10), 1938-1956.

Russell, R. G., Watts, N. B., Ebetino, F. H., & Rogers, M. J. (2008). Mechanisms of action of bisphosphonates: similarities and differences and their potential influence on clinical efficacy. *Osteoporos Int, 19*(6), 733-759. doi:10.1007/s00198-007-0540-8

Sato, M., Grasser, W., Endo, N., Akins, R., Simmons, H., Thompson, D. D., . . . Rodan, G. A. (1991). Bisphosphonate action. Alendronate localization in rat bone and effects on osteoclast ultrastructure. *J Clin Invest, 88*(6), 2095-2105. doi:10.1172/JCI115539

Scheper, M. A., Badros, A., Salama, A. R., Warburton, G., Cullen, K. J., Weikel, D. S., & Meiller, T. F. (2009). A novel bioassay model to determine clinically significant bisphosphonate levels. *Support Care Cancer, 17*(12), 1553-1557. doi:10.1007/s00520-009-0710-7

Singhatanadgit, W., Hankamolsiri, W., & Janvikul, W. (2021). Geranylgeraniol prevents zoledronic acid-mediated reduction of viable mesenchymal stem cells via induction of Rho-dependent YAP activation. *R Soc Open Sci, 8*(6), 202066. doi:10.1098/rsos.202066

Tavares Ddos, S., Castro Lde, O., Soares, G. D., Alves, G. G., & Granjeiro, J. M. (2013). Synthesis and cytotoxicity evaluation of granular magnesium substituted beta-tricalcium phosphate. *J Appl Oral Sci, 21*(1), 37-42. doi:10.1590/1678-7757201302138

Thousand, J., Datar, J., Font, K., & Powell, C. A. (2017). A root volume study of the adult dentition for ridge preservation purposes. *Gen Dent, 65*(5), 21-23. Retrieved from https://www.ncbi.nlm.nih.gov/pubmed/28862584

Vaisman, D. N., McCarthy, A. D., & Cortizo, A. M. (2005). Bone-specific alkaline phosphatase activity is inhibited by bisphosphonates: role of divalent cations. *Biol Trace Elem Res, 104*(2), 131-140. doi:10.1385/bter:104:2:131

Wen, D., Qing, L., Harrison, G., Golub, E., & Akintoye, S. O. (2011). Anatomic site variability in rat skeletal uptake and desorption of fluorescently labeled bisphosphonate. *Oral diseases, 17*(4), 427-432. doi:10.1111/j.1601-0825.2010.01772.x